AJNR

Diffusion Imaging in Obstructive Hydrocephalus

Aziz M. Ulug, Thuy N. Truong, Christopher G. Filippi, Terry Chun, Jimmy K. Lee, Charles Yang, Mark M. Souweidane and Robert D. Zimmerman

AJNR Am J Neuroradiol 2003, 24 (6) 1171-1176
http://www.ajnr.org/content/24/6/1171

AJNR Am J Neuroradiol 24:1171–1176, June/July 2003

Diffusion Imaging in Obstructive Hydrocephalus

Aziz M. Uluğ, Thuy N. Truong, Christopher G. Filippi, Terry Chun, Jimmy K. Lee, Charles Yang, Mark M. Souweidane, and Robert D. Zimmerman

BACKGROUND AND PURPOSE: **Hydrocephalus causes transependymal resorption of spinal fluid that in turn produces periventricular interstitial edema. This study was performed to determine if diffusion imaging can demonstrate this interstitial edema in the periventricular region in patients with obstructive hydrocephalus and if it can be used to assess the treatment response.**

METHODS: **Twenty-one patients with obstructive hydrocephalus were evaluated with MR diffusion imaging before and after treatment. The change in ventricular size was measured by using the frontal and occipital horn ratio. The signal intensity abnormalities in periventricular white matter were scored. Average diffusion constants (D_{av}) in the periventricular white matter were measured before and after treatment and compared with normal values. Post-treatment resolution of MR imaging abnormalities and changes in ventricular volume were compared with changes in D_{av}.**

RESULTS: **D_{av} measured from periventricular white matter was increased in hydrocephalic patients compared with age-matched control subjects by a mean of 6.9% ($P < .02$). After treatment, D_{av} decreased by an average of 6.0%: D_{av} decreased in 11 patients (53%), it remained essentially unchanged in seven (33%), and it increased in three (14%).**

CONCLUSION: **For patients with obstructive hydrocephalus, diffusion is usually increased in the periventricular white matter. Therefore, increased D_{av} may be a clinically useful sign of hydrocephalus, and it may prove useful in cases with equivocal clinical or imaging findings. Measurement of D_{av} may be valuable in assessing the treatment response in these patients because D_{av} usually decreases toward normal levels with successful treatment.**

Normal CSF dynamics is a balance between the production and resorption of spinal fluid. Pathologic processes can occur anywhere along the normal pathway of CSF flow and disrupt this balance. Left untreated, this condition can lead to severe neurologic dysfunction and death (1, 2).

CT and MR imaging studies are instrumental in the assessment of hydrocephalus. Typical features include ventricular dilatation and periventricular white matter edema due to the transependymal resorption of spinal fluid (3–9). However, imaging features may be inconclusive. These findings are not always reliable indicators of hydrocephalus because ventricular dilatation and periventricular hyperintensity (PVH) are routinely seen in elderly patients (7, 9–11), whereas some hydrocephalic patients have only mild ventricular dilatation without PVH (9).

Some have postulated that the diffusion of water in the periventricular region should be increased because of the transependymal resorption of CSF. This process produces an increase in the extracellular water content in the adjacent tissue (interstitial edema). Increased diffusion in the periventricular region has been documented in an animal model (12) and in selected clinical cases of normal-pressure hydrocephalus (13–15). We hypothesize that the average diffusion constants (D_{av}) of the periventricular white matter increases in obstructive hydrocephalus as a result of this excess extracellular water. In this article, we evaluated the effectiveness of diffusion-weighted (DW) imaging and the quantification of D_{av} in identifying periventricular interstitial edema associated with hydrocephalus and in assessing the treatment outcome.

Methods

Twenty-one patients with obstructive hydrocephalus were examined. Patients were included in the study when 1) clinical and morphologic imaging findings characteristic for hydrocephalus were present, 2) patients were to undergo treatment for the hydrocephalus, and 3) clinical symptoms of hydrocephalus resolved after treatment. At the time of the first MR measurement, patients ranged in age from 80 days to 67 years

Received July 17, 2002; accepted after revision, January 1, 2003.

From the Departments of Radiology (A.M.U., T.N.T., C.G.F., T.C., C.Y., R.D.Z.) and Neurosurgery (J.K.L., M.M.S.), Weill Medical College of Cornell University, New York, NY.

Address correspondence to Aziz M. Uluğ, PhD, Weill Medical College of Cornell University, Department of Radiology, Box 141, 1300 York Avenue, New York, NY 10021.

TABLE 1: Diagnosis, age, and time between D_{av} measurement and treatment in patients with hydrocephalus

Patient	Diagnosis	Age, y	Time Between First Measurement and Treatment, d	Time Between Second Measurement and Treatment, d
1	Choroid plexus papilloma	0.2	3	3
2	Vein of Galen malformation	0.5	9	4
3	Pineal tumor	1.5	1	3
4	Choroid plexus papilloma	2.0	2	6
5	Medulloblastoma	2.1	0*	2
6	Juvenile pilocytic astrocytoma	3.1	2	0*
7	Medulloblastoma	3.4	1	11
8	Subependymal giant cell astrocytoma	4.2	4	2
9	Diencephalic cyst	5.6	2	3
10	Juvenile pilocytic astrocytoma	7.1	0*	1
11	Ependymoma	8.0	1	0*
12	Cerebellar astrocytoma	8.8	1	2
13	Medulloblastoma	8.9	13	5
14	Medulloblastoma	9.2	1	1
15	Juvenile pilocytic astrocytoma	11.3	1	3
16	Hypothalamic glioma	13.9	1	8
17	Aqueduct stenosis	15.9	4	1
18	Aqueduct stenosis	19.6	2	1
19	Primary glioma	22.0	1	0*
20	Aqueduct stenosis	50.4	9	1
21	Colloid cyst of third ventricle	67.5	6	2
Mean		12.6	3.0	2.8
SD		16.8	3.4	2.8

* Same day.

(mean, 13 years ± 17). The causes of hydrocephalus included neoplasms (15 of 21), congenital and non-neoplastic abnormalities (six of 21), or vascular malformations (one of 21). All patients were imaged before and after treatment. The time between the first measurement and treatment was less than 2 weeks (range, 0–13 days). The initial post-treatment MR image was obtained within 2 weeks of treatment (range, 0–11 days). The diagnosis and the time between measurements for each patient are listed in Table 1. Nine patients were imaged more than once after treatment, and one patient (patient 2) was imaged twice before treatment and three times after treatment.

All studies were conducted by using a 1.5-T whole-body MR imager (GE Signa; General Electric Medical Systems, Milwaukee, WI) equipped with high-performance gradients by using a manufacturer-supplied quadrature head coil. In all patients, sagittal T1-weighted (TR/TE/NEX, 300/14/1), axial fast spin-echo T2-weighted (3000/91/1), and axial fast fluid-attenuated inversion recovery (FLAIR) (10002/172/1) images were obtained with a null time of 2200 ms. In general, all routine axial sequences used a section thickness of 5 mm, a 256 × 192 matrix, and a 22-cm FOV. All patients were imaged with a diffusion-weighted echo-planar multisection sequence (TR/TE, 10,500/102). Diffusion was measured in three directions (x, y, z) with a b value of 1000 s/mm^2 for each axis. In addition, an image without diffusion gradients was obtained. A matrix of 128 × 128 was used for all diffusion images with an FOV of 22 cm and a section thickness of 5 mm.

Routine MR images were evaluated for the presence of hydrocephalus by using standard techniques. We assessed the size of the ventricle before and after treatment by measuring the frontal and occipital horn ratio (FOR), which was the ratio of the width of the frontal horns plus the width of the occipital horns divided by twice the interparietal diameter. This technique has been shown to be reliable method for estimating ventricular volume (16). PVH was graded (9) on FLAIR images, as follows: 0, none; 1, discontinuous with foci seen adjacent to the frontal and occipital horns of the lateral ventricles; 2, continuous with a pencil-thin continuous line around the ventricles; 3, periventricular halo with a band of hyperintensity with smooth peripheral margins surrounding the ventricles; and 4, diffuse abnormality with hyperintensity extending from the ventricular margins into the surrounding white matter with irregular peripheral margins. On the basis of previous experience (9), patterns 3 and 4 are considered to represent transependymal resorption of CSF due to hydrocephalus, whereas patterns 0–2 are either normal or nonspecific.

These MR imaging abnormalities associated with hydrocephalus (ventricular dilatation and PVH) were correlated with the changes in the diffusion constant and with diffusion measurements before and after treatment.

To measure the pre- and post-treatment D_{av} values, an orientation independent diffusion map was calculated for each pixel from the DW images, as follows: D_{av} = trace/3 = (Dxx + Dyy + Dzz)/3. For each patient, D_{av} values were then calculated from regions of interest (ROIs) placed over the periventricular white matter (Fig 1). In determining D_{av} for each patient, we used 25–60 ROIs in multiple sections (two to three sections at the level of the lateral ventricles). Values were obtained from the periventricular region in areas that appeared isointense relative to normal white matter on the diffusion maps. The pre- and post-treatment D_{av} values were compared with determine the percentage change in D_{av} with treatment.

Additionally, pre- and post-treatment D_{av} values were compared with normative D_{av} values. Normal values of D_{av} for white matter were calculated from data in 38 adult volunteers and 26 pediatric patients without hydrocephalus from our previous studies (17–19).

Pre- and post-treatment D_{av} values and pre- and post-treatment FOR values were compared by using a paired Student t test. We also compared the change in FOR with the change in D_{av}. The significance level was set at $P < .05$.

Results

Values of D_{av}, FOR, and PVH are summarized in Table 2. FOR values decreased by an average of 7.4% after treatment; this was indicative of the resolution

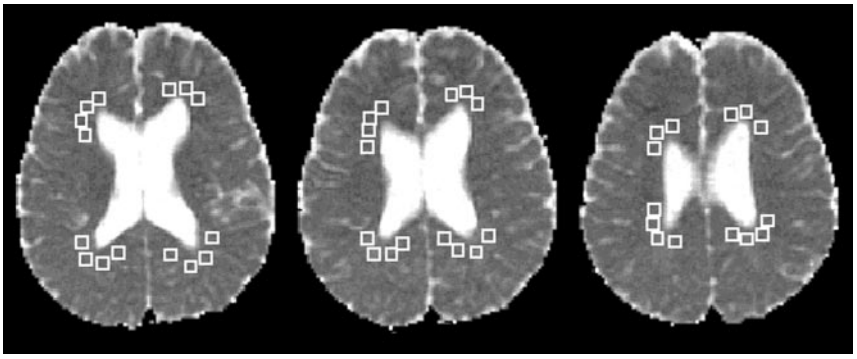

FIG 1. Patient 6. ROIs chosen to measure periventricular D_{av} values are shown on D_{av} maps. The D_{av} value determined from 44 periventricular white matter ROIs was 0.85 10^{-5} cm^2/s (third MR examination).

TABLE 2: D_{av}, FOR, and PVH values before and after treatment and percentage change

	$D_{av} \times 10^{-5}$ cm^2/s		Change in D_{av}, %			FOR Value			PVH Value	
Case	Before Treatment	After Treatment	Before Treatment vs After Treatment*	Before Treatment vs Normal†	After Treatment vs Normal‡	Before Treatment	After Treatment	Change, %§	Before Treatment	After Treatment
1	1.46	1.15	−21.2	25.6	0.1	0.64	0.50	−29.3	2	0
2	1.28	1.12	−12.5	20.5	5.9	0.45	0.44	−2.7	0	1
3	1.17	1.00	−14.5	17.1	0.1	0.58	0.46	−24.1	4	3
4	1.08	0.87	−19.4	10.9	−10.6	0.46	0.41	−12.7	1	1
5	0.85	0.92	8.2	−12.5	−5.3	0.37	0.36	−2.9	2	2
6	0.88	0.91	3.4	−5.6	−2.4	0.40	0.41	1.7	3	3
7	0.87	0.88	1.1	−5.7	−4.6	0.33	0.31	−4.5	2	2
8	0.82	0.79	−3.7	−8.7	−12.0	0.43	0.33	−31.5	3	2
9	0.85	0.84	−1.2	−1.7	−2.8	0.54	0.49	−9.6	3	3
10	0.98	0.92	−5.3	17.0	10.8	0.49	0.45	−7.9	2	2
11	0.79	0.79	0.0	−4.4	−4.4	0.37	0.36	−4.7	2	2
12	0.85	0.82	−3.5	4.9	1.2	0.47	0.48	2.1	3	3
13	0.79	0.80	1.3	−2.5	−1.2	0.35	0.34	−2.6	2	2
14	0.84	0.83	−1.2	4.1	2.9	0.44	0.40	−9.6	2	2
15	0.89	0.80	−9.9	13.0	1.9	0.42	0.40	−5.0	2	2
16	0.79	0.78	−1.3	2.4	1.1	0.41	0.39	−3.3	2	2
17	0.92	0.78	−15.2	20.4	2.1	0.51	0.50	−1.3	3	1
18	0.99	0.73	−26.3	31.0	−3.4	0.43	0.46	6.6	2	1
19	0.84	0.78	−6.9	11.3	3.6	0.39	0.38	−2.7	3	3
20	0.80	0.79	−1.3	7.1	5.8	0.53	0.48	−9.1	2	2
21	0.75	0.77	2.7	0.4	3.1	0.49	0.48	−2.5	2	2
Mean	0.93	0.86	−6.0	6.9	−0.4	0.45	0.42	−7.4	2.2	2.0
SD	0.18	0.11	9.1	12	5.3	0.08	0.06	9.8	0.8	0.8

* $P < .007$
† $P < .02$
‡ $P > .64$
§ $P < .003$

of ventriculomegaly caused by hydrocephalus. After treatment, FOR decreased in 11 patients, it remained fairly constant in nine patients, and it increased in one patient. The difference between pre- and post-treatment FOR values was statistically significant ($P < .003$).

The average PVH was 2.2 on the initial examination and decreased to 2.0 after treatment. After treatment, PVH slightly increased in one patient, it did not change in 15 patients, and it decreased in five patients. PVH was not a reliable indicator of hydrocephalus or the treatment response.

The average D_{av} decreased by 6.0% after treatment. The average D_{av} at different times was plotted for select patients (Fig 2). Post-treatment D_{av} values decreased in 11 patients, they remained relatively constant in seven patients, and they increased in three patients. The highest percentage change between pre- and post-treatment values was 26% (patient 18). Post-treatment D_{av} was significantly lower than pretreatment D_{av} ($P < .007$). In the patients in whom the pretreatment D_{av} was normal or decreased, the post-treatment values did not decrease further.

Pretreatment D_{av} measured from periventricular white matter was, on average, 6.9% higher in hydrocephalic patients than in normal control subjects. Results of the paired t test showed a statistically significant difference between the pretreatment D_{av} and the normative D_{av} values ($P < .02$). The post-treatment D_{av} results were not significantly different from the normative values ($P > .64$) as a group; this finding

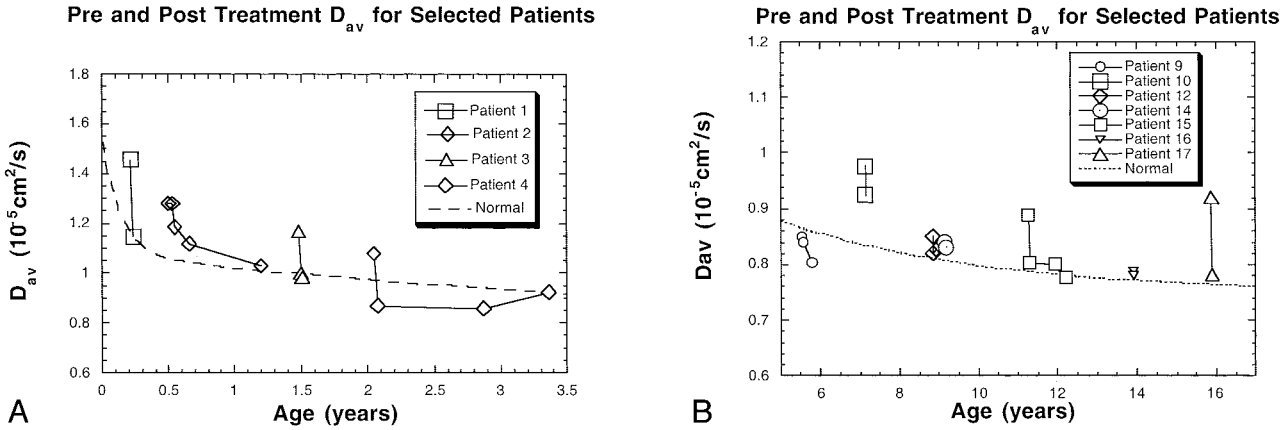

FIG 2. Pre- and post-treatment periventricular white matter D_{av} measurements in select patients are displayed relative to values in age-matched control subjects. The *dotted line* indicates normative values from references 18 and 19.
A, Patients 1–4.
B, Patients 9, 10, 12, and 14–17.

suggested successful treatment. In the nine patients who were imaged multiple times after treatment, the diffusion values stabilized to normal levels.

When the change in FOR was compared with the change in D_{av}, a linear correlation was observed. A decrease in the ventricular size correlated with a decrease in the D_{av} in periventricular white matter. This correlation, however, was not statistically significant in this patient population ($P > .35$).

Discussion

In certain clinical situations, the diagnosis of hydrocephalus may be difficult to establish, particularly in the very young or the very old. The ventricles and sulci diminish in size (relative to the overall intracranial volume) during the first 2 years of life as the brain matures. Therefore, differentiating normal ventricles from mildly dilated ventricles may be difficult (3). The open cranial sutures alter the pressure and volume dynamics of the intracranial space in the presence of hydrocephalus, leading to variable enlargement of the ventricles and sulci. In elderly patients, atrophy routinely causes some degree of ventricular dilatation. Therefore, the presence of concomitant atrophy and hydrocephalus can limit the diagnostic accuracy of CT and MR imaging (7, 10, 11).

The cases in this series were specifically chosen because the clinical and morphologic findings of hydrocephalus were clear cut, and yet, grade 3 or 4 PVH was seen in only seven of 21 cases. After treatment, PVH decreased in five patients and increased in one patient. The results show the ineffectiveness of using PVH to assess obstructing hydrocephalus and the effects of treatment.

In animal experiments (12) and in a limited number of patients with normal-pressure hydrocephalus (13–15) increased diffusion has been identified with DW imaging. Our results provide support for this hypothesis. Diffusion, as measured by D_{av}, was increased (relative to age-corrected normal values) in the periventricular white matter in areas where no signal intensity abnormalities were seen on FLAIR and T2-weighted images. Abnormal signal intensity was not visible on DW images or on diffusion maps. Therefore, the detection of increased diffusion required the measurement of D_{av} from the diffusion maps. The pretreatment changes in D_{av} ranged from –12.5% to 31.0%, relative to normal values. This variation probably reflects the extent of subependymal absorption of CSF in these patients. Hydrocephalus is a complex, dynamic process. Factors such as the site and cause of obstruction, the duration of disease, and the patient's age may affect the degree to which transependymal resorption and other compensatory mechanisms occur in individual patients. In this small series, an assessment of the potential causes of the variation in transependymal absorption was not possible. In the future, the evaluation of data from diffusion imaging may improve our understanding of the compensatory mechanisms that occur in hydrocephalus, and it may aid in treatment planning.

The extent of the decrease in D_{av} was determined by the extent of the elevation of D_{av} before treatment. This decrease occurred rapidly. Serial studies in nine patients revealed that D_{av} decreased continued to normalize, then remained normal for their age over time (Figs 2 and 3). In the few cases in which the pretreatment study did not show interstitial edema (ie, normal D_{av}, post-treatment values) were not expected to change. Regardless of the initial values, successful treatment resulted in the normalization of D_{av}.

In two cases, morphologic evidence showed incomplete decompression of the ventricular system; this was well correlated with D_{av} measurements. Patient 2 was an infant in whom a vein of Galen malformation was successfully occluded via an endovascular approach without surgical decompression of the ventricular system. The initial post-treatment MR study demonstrated a mild decrease in both ventricular size and $D_{av.}$ Subsequent MR imaging performed 7 weeks later revealed a further decrease in both ventricular size and D_{av}. An examination at 7 months demonstrated a further decrease in D_{av} that paralleled the

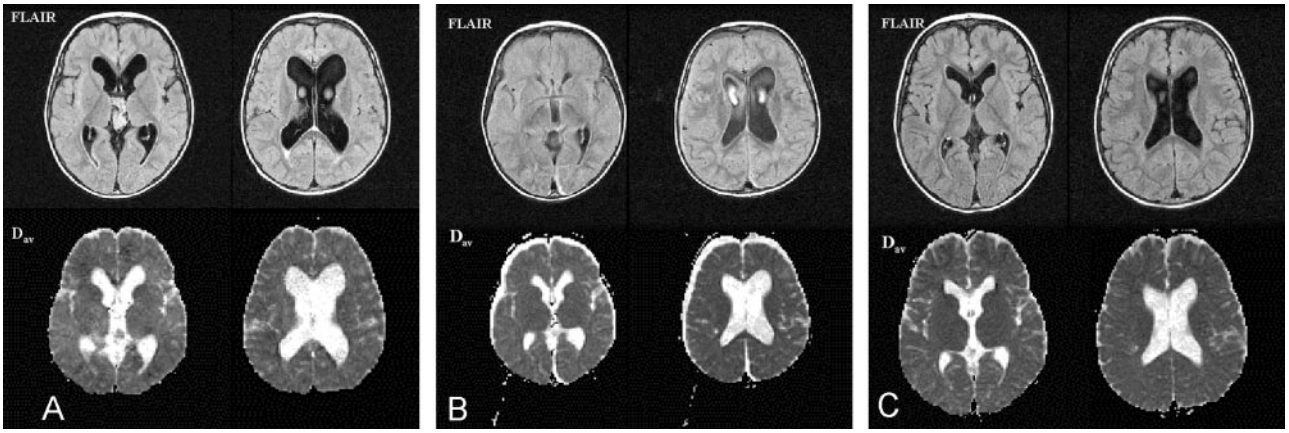

FIG 3. Patient 4. Pre- and post-treatment images in a patient with a third ventricular choroid plexus papilloma.

A, Pretreatment FLAIR images at the level of the foramen of Monro and the lateral ventricles (*top row*) reveal the presence of the third ventricular choroid plexus papilloma. Ventricular dilatation and a grade 1 PVH are present. The D_{av} value was 1.08, 21% above normal. D_{av} maps at the corresponding levels (*bottom row*) show no evidence of abnormal signal intensity in the periventricular region.

B, Post-treatment images obtained on day 6 after tumor resection. On the FLAIR images (*top row*), the ventricles are smaller than before, and the PVH has decreased. Postoperative subdural collections are present. The D_{av} value has decreased to 0.87 (19% change) (*bottom row*).

C, Subsequent FLAIR images obtained 7 months after surgery reveal no evidence of tumor recurrence (*top row*). Subdural collections have resolved. The D_{av} value is 0.85, which is normal for the patient's age (*bottom row*).

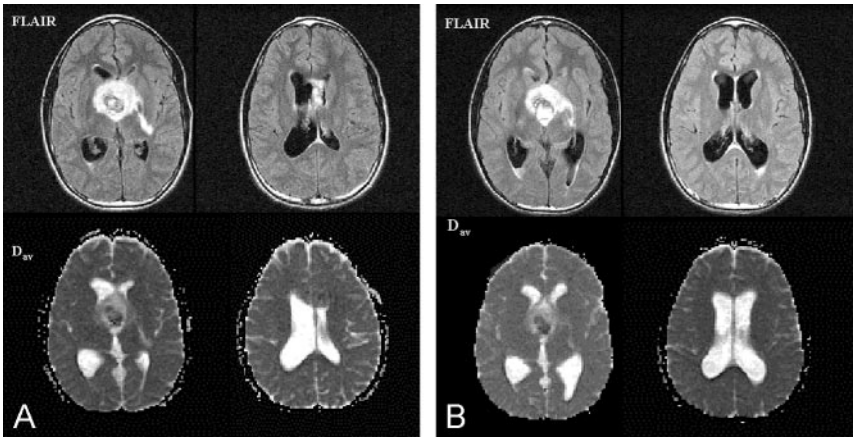

FIG 4. Patient 16. Pre- and post-treatment images in a 13-year-old patient with a malignant hypothalamic glioma.

A, Pretreatment FLAIR images (*top row*) reveal the hypothalamic mass, hydrocephalus with symmetric dilatation of the lateral ventricles, and a grade 2 PVH. D_{av} images (*bottom row*) demonstrate normal-appearing periventricular white matter. The D_{av} value was 0.79, only 3% above normal for the patient's age.

B, Repeat MR study was performed 7 days after partial resection and shunt placement. FLAIR images (*top row*) reveal residual tumor in the hypothalamus and asymmetric ventricular dilatation. The left lateral ventricle is smaller, but the right lateral ventricle is larger, consistent with unilateral obstruction at the foramen of Monro. The D_{av} value was also asymmetric (*bottom row*). In the left periventricular white matter, it had decreased to 0.76, whereas in the right periventricular white matter, it had increased to 0.80.

normal decrease seen in the first year of life (Fig 2). In a second case (patient 16), a hypothalamic glioma was resected and a shunt was inserted. The postsurgical MR images revealed decompression of the left lateral ventricle but increased dilatation of the right lateral ventricle indicative of unilateral obstruction at the foramen of Monro (Fig 4). The mean D_{av} was 0.78, but the D_{av} of the right periventricular white matter was 0.80, whereas that of the left periventricular white matter was 0.76. These findings indicated that the shunt was not adequately decompressing the right lateral ventricle. After shunt revision, the lateral ventricles became symmetric.

In this patient group, the change in ventricular size (FOR value) and the change in the D_{av} of the periventricular white matter was statistically significant after successful treatment. Interestingly, when we correlated these changes with each other, we found a linear relation, as expected. This result showed that, after successful treatment, ventricular size and periventricular white matter D_{av} both decreased. However, this correlation was not statistically significant, possibly because the information given by D_{av} and the ventricular size was in fact different. The information given by the ventricular size measurements (FOR values) is morphologic and more related to the increased CSF pressure than to the tissue response. On the contrary, the information given by the periventricular white matter D_{av} is related to the status of tissue microstructure, and as such, it may be better correlated with the clinical symptoms.

Our study results indicate that diffusion imaging may prove useful in the initial assessment and in the post-treatment monitoring of patients with hydrocephalus. It is important to note the potential limitations of this technique. In some patients with hydrocephalus, transependymal resorption of CSF may be minimal, and therefore, elevation of D_{av} is mild or absent. The increased diffusion is not appreciable by

means of visual inspection of DW images or diffusion maps. Measurement of D_{av} in the periventricular white matter is required. The D_{av} must be compared with data from healthy age-matched patients, at least during the pretreatment examination. The normal D_{av} of periventricular white matter is highly age dependent in young children (19). In young children, the change in D_{av} after treatment may be more important than the absolute value. Care must also be taken in evaluating the importance of changes in D_{av} over long periods in children younger than 2 years, because this measurement dramatically decreases with normal brain maturation. D_{av} remains relatively constant throughout the remainder of one's lifetime, increasing slightly after the age of 60 years (18). A comparison of D_{av} values before and after treatment should suffice, as our results demonstrated that D_{av} decreases within a few days of successful treatment. On the basis of our findings, we recommend that D_{av} be measured several days after treatment. This value can then serve as an internal baseline reference for subsequent examinations. A subsequent elevation of D_{av} above this internal baseline may be a sign of recurrent hydrocephalus.

Conclusion

We used diffusion imaging to detect periventricular interstitial edema due to transependymal resorption of spinal fluid in hydrocephalic patients. The diffusion constant D_{av} was elevated relative to normal values in age-matched control subjects as a group (average, 6.9%). After successful treatment, the diffusion constant rapidly decreased (average decrease, 6.0%). This technique may prove useful in cases in which the clinical and morphologic imaging findings are not diagnostic. Changes in D_{av} may be a better indicator of the treatment response than the ventricular size or the signal intensity changes in the periventricular white matter.

Acknowledgments

We thank the competent MR technologists of New York Presbyterian Hospital for performing imaging studies in the patients presented herein.

References

1. Schurr PH, Polkey CE. *Hydrocephalus.* London: Oxford University Press; 1993
2. Rekate HL. **Recent advances in the understanding and treatment of hydrocephalus.** *Semin Pediatr Neurol* 1997;4:167–178
3. Barkovich, AJ. *Pediatric Neuroimaging* 2nd ed. Philadelphia: Lippincott-Raven; 1996:439–475
4. Tavaras JM, Woods EH. *Diagnostic Neuroradiology* 2nd ed. Baltimore: Williams and Wilkins; 1976:101–102
5. Gunasekera L, Richardson AE. **Computerized axial tomography idiopathic hydrocephalus.** *Brain* 1977;100:749–754
6. Quisling RQ, Peters KR. **Computed tomography.** In: Youmans JR, ed. *Neurological Surgery* 4th ed. Philadelphia: Saunders; 1996:101–105
7. Bradley WM, Quencer RM. **Hydrocephalus and cerebrospinal fluid flow.** In: Stark DD, Bradley WM eds. *Magnetic Resonance Imaging* 3rd ed. St Louis: Mosby; 1999:1483–1507
8. El Gammal T, Allen MB Jr, Brooks BS, Mark ED. **MR evaluation of hydrocephalus.** *AJNR Am J Neuroradiol* 1987;8:591–597
9. Zimmerman RD, Fleming CA, Lee BCP, Saint-Louis LA, Deck MDF. **Periventricular hyperintensity as seen by magnetic resonance: prevalence and Significance.** *AJR Am J Roentgenol* 1986;146:443–450
10. Jack CR, Mokri B, Laws ER Jr, et al. **MR findings in normal-pressure hydrocephalus: significance and comparison with other forms of dementia.** *J Comput Assist Tomogr* 1987;11:923–931
11. Bradley Jr. WG. Commentary. **MR prediction of shunt response in NPH: CSF morphology versus physiology.** *AJNR Am J Neuroradiol* 1998;19:1285–1286
12. Ebisu T, Naruse S, Horikawa Y, et al. **Discrimination between different types of white matter edema with diffusion-weighted MR imaging**. *JMRI* 1993;863–868
13. Gideon P, Thomsen C, Gjerris F, Sorensen PS, Henriksen O. **Increased self-diffusion of brain water in hydrocephalus measured by MR imaging.** *Acta Radiologica* 1994;35:514–519
14. Chun T, Filippi CG, Relkin N, Zimmerman RD, Uluğ AM. **Diffusion changes in Normal Pressure Hydrocephalus.** *Proc Intl Soc Magn Reson Med* 2000;8:797
15. Uluğ AM, Relkin N, Zimmerman RD. **Diagnosis of normal pressure hydrocephalus using diffusion imaging.** In: International Proceedings of the 30th Annual Meeting of the American Aging Association. Madison: American Aging Association; 2001:72
16. O'Hayon BB, Drake JM, Ossip MG, Tuli S, Clarke M. **Frontal and occipital horn ratio: a linear estimate of ventricular size for multiple imaging modalities in pediatric hydrocephalus.** *Pediatr Neurosurg* 1998;29:245–249
17. Uluğ AM, Filippi CG, Souweidane M, Zimmerman RD. **Use of diffusion imaging for assessing the treatment of obstructive hydrocephalus.** *Proc Intl Magn Reson Med* 1999;7:923
18. Chun T, Filippi CG, Zimmerman RD, Uluğ AM. **Diffusion changes in the aging human brain.** *AJNR Am J Neuroradiol* 2000;21:1078–1083
19. Uluğ AM. **Monitoring brain development with quantitative diffusion tensor imaging.** *Dev Sci* 2002;5:3:286–292